DOI: 10.13009/EUCASS2017-350

Effective Plasma Buffet and Drag Control for Laminar Transonic Aerofoil

Pavel A. Polivanov, Andrey A. Sidorenko and Anatoly A. Maslov
Khristianovich Institute of Theoretical and Applied Mechanics SB RAS
630090, Institutskaya, 4/1, Novosibirsk, Russia
polivanov@itam.nsc.ru

Abstract

The effect of plasma actuators on Shock Wave / Laminar Boundary Layer Interaction (SWBLI) was studied experimentally on transonic laminar aerofoil. The unsteady characteristics of the separation zone including the transonic buffet were measured. Two kinds of electrical discharge actuators were used for the flow control. Successful suppression of separated flow and laminar transonic buffet by plasma actuators was demonstrated. An analysis of the effect of power and frequency of the discharge on SWBLI was carried out. High efficiency ratio of the separation control by plasma actuators was achieved in the experiments.

1. Introduction

It is commonly accepted that laminar transonic aerofoil should allow to significantly improve the efficiency of transonic aircraft of the next generation. However the features of flow separation at the shock wave / laminar boundary layer interaction (SWBLI) are significantly different from the turbulent cases and not well studied. For example, in papers [1, 2] the characteristics of a laminar transonic aerofoil were studied and natural laminar-turbulent transition was detected in the separation bubble for wide range of the angle of attack. The turbulization of the boundary layer inhibited the growth of the laminar bubble, which positively affects the aerofoil performance. The mode of transonic buffet for a laminar regime is featured by smaller amplitude and a significantly higher frequency of the shock wave oscillations in comparison with the turbulent case. In more detail, the physics of the phenomenon was studied for the test case of flat plate with incident oblique shock wave at small supersonic Mach numbers with in [3, 4, 5]. Despite the small differences in these experimental studies, the main results are similar: the turbulent boundary layer does not reduce the drag in the interaction zone; in the laminar bubble pulsations rapidly increase leading to turbulence of the flow; in the laminar bubble complex nonstationary phenomena occur, most probably as a result of the growth of the disturbances due to the intrinsic instability of the separation bubble and shear layer. These conclusions are confirmed by the results of numerical simulation [6, 7].

The analysis reveals that the unsteady phenomena for the laminar case develop differently than for the turbulent one. Therefore, not all methods of the separated flow control developed for transonic turbulent aerofoils [8] can be suitable for laminar aerofoils. In [9] it was proposed to use a turbulator of special type to improve the resistance of the aerofoil to laminar transonic buffet. The numerical simulations confirm the possibility of suppressing the buffet, but at the same time the lifting performance of the aerofoil decreases. To maintain the advantages of a laminar aerofoil it is proposed to make a retractable turbulator but this will greatly complicate the design.

In paper [5] it was found that the minimum size of the zone of SWBLI and low level of pulsations may be achieved if the state of inflow boundary layer corresponds to the beginning of the laminar-turbulent transition (low level of intermittency). Since the electrical discharge may introduce disturbances in the laminar boundary layer with predetermined intermittency, it was decided apply this control technique and to study the effect of plasma actuators on separated flows on laminar transonic aerofoil.

2. Experimental setup

The experiments were performed in wind tunnel T-325 (ITAM SB RAS) for Mach number M_∞ = 0.68-0.72, T_0 = 290 K and P_0 = 0.3-0.7·10^5 Pa. Figure 1 shows the model installed in the wind tunnel test section. The model was optimized for conditions of the test section of T-325. The main purpose of optimization was to reduce the influence of the sidewalls and to maximize the model chord to improve the accuracy of quantitative measurements. As the base point of optimization of the model shape we have chosen the transonic NLF airfoil [10]. During the numerical optimization process more than 10 configurations of the experimental models were considered.

DOI: 10.13009/EUCASS2017-350

The following measuring methods were used: PIV, unsteady pressure sensors, high-speed Schlieren and IR visualization. Detailed measurements of steady and unsteady characteristics of the separation zone were performed. Two new types of plasma actuators have been developed: MSSD (Multi Sliding Spark Discharge) and CDBD (Contracted Dialectical Barrier Discharge). Schematically MSSD and CDBD configurations are shown in Figure 2. The experiments revealed that these two types of discharge demonstrate the same effect for the same energy in the pulse, therefore only CDBD is considered further. CDBD is a new plasma actuator specially designed for the introduction of disturbances in the boundary layer. This discharge may be simply integrated into the aircraft structure, operating at moderate voltage and does not require expensive/heavy power supplies.
To ensure smooth contours of the model the actuators were milled by CNC from MACOR and the models body was made of PEEK. Sensors Honeywell SCCP15GSMT were used to measure the pressure fluctuations on the wall. The sensors were placed in-line on the same distance from the leading edge (x = 162 mm) to study 3D features of the shock wave oscillations.

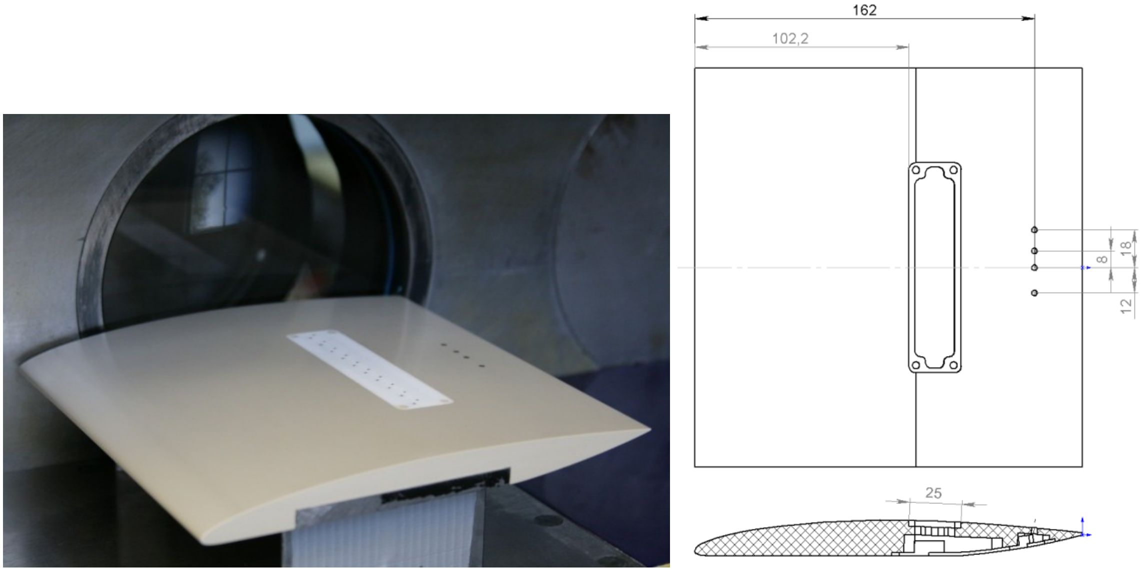

Figure 1: Photo and draft of the model

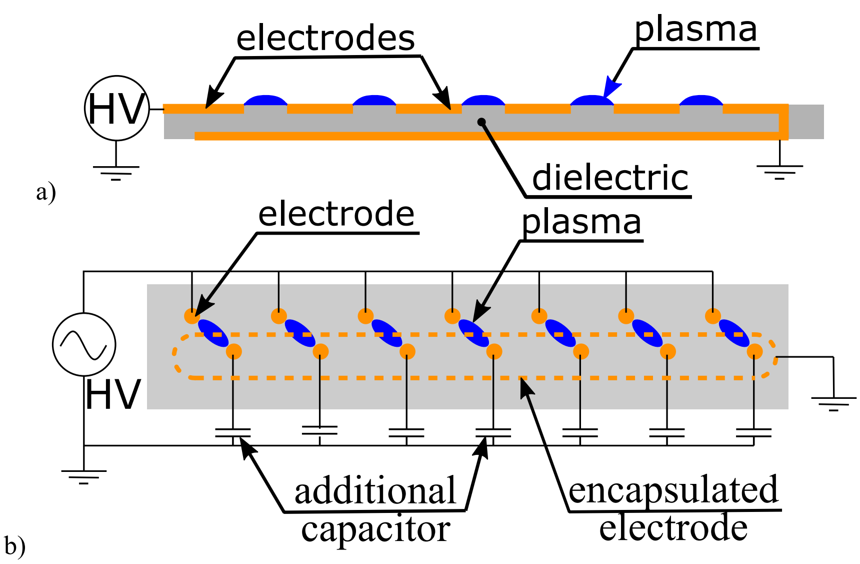

Figure 2: Schematic of a) MSSD and b) CDBD

DOI: 10.13009/EUCASS2017-350

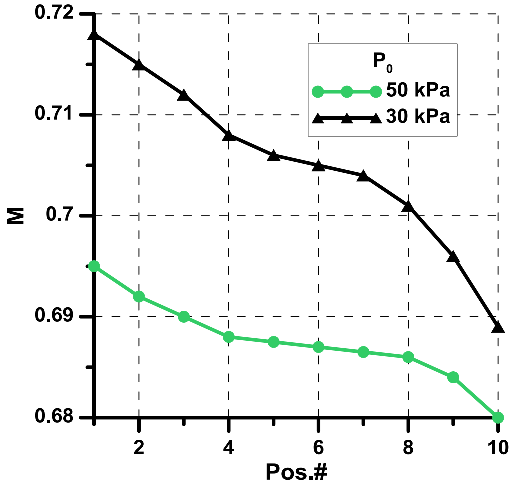

Figure 3: Free stream Mach number vs. elliptic shaft position

Free stream Mach number was calculated basing on the total pressure P_0 and the static pressure P_{st} measured on the test section wall upstream of the model. These data are presented in Figure 3 for various positions of the elliptic shaft controlling the second throat section of the test chamber. It can be seen that free stream Mach number value was about 0.7 and slightly increased with decreasing of pressure.
Waveforms of current and voltage measured on CDBD actuator are shown in Figure 4. Comparison of these waveforms with the waveforms of classical DBD shows that the breakdown (sharp spikes of the current) occurs much rarely due to fine tuning of the breakdown conditions for each gap by additional capacitor. In fact, the breakdown for each individual electrode pair occurs twice for the period, but due to some differences of discharge gaps characteristics and local conditions the breakdowns of all the gaps are not simultaneous.

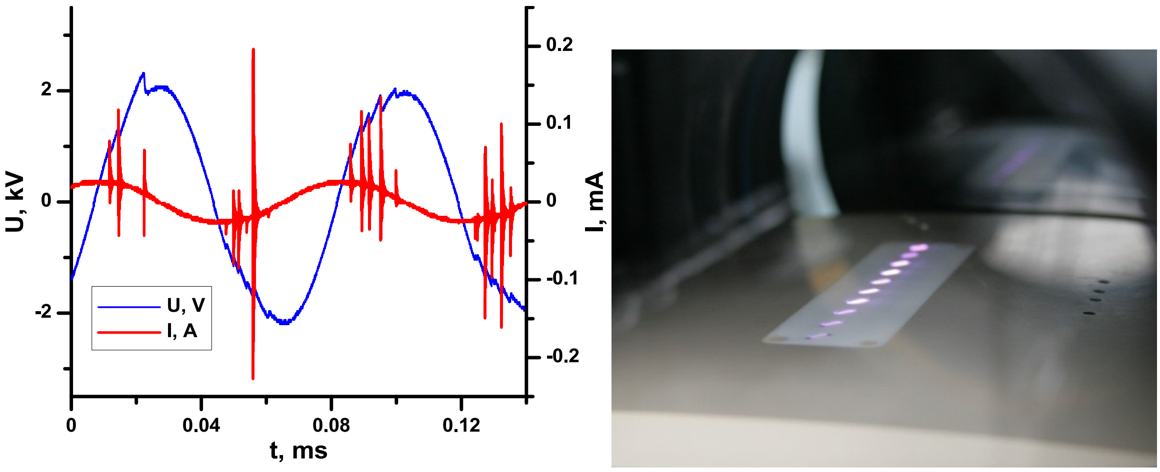

Figure 4: Waveforms of the voltage and current on CDBD actuator and photo of the actuator

3. Experimental results

Examples of Schlieren images obtained are presented in Figure 5 and Figure 6 (flow from the left to the right). It is clearly seen that the laminar boundary layer is maintained upstream of the interaction zone not only at low pressure P_0 = 0.3 bar, but also at higher P_0 = 0.7 bar. This result has been confirmed by thermal imaging visualization. Nevertheless, the small flow distortion caused by imperfections of polishing of the MACOR inserts can be found on visualization. For example, in the Schlieren image obtained for P_0 =0.7 bar a weak perturbation is clearly seen at the insert's front edge followed by weak shock wave at the end of the insert.

DOI: 10.13009/EUCASS2017-350

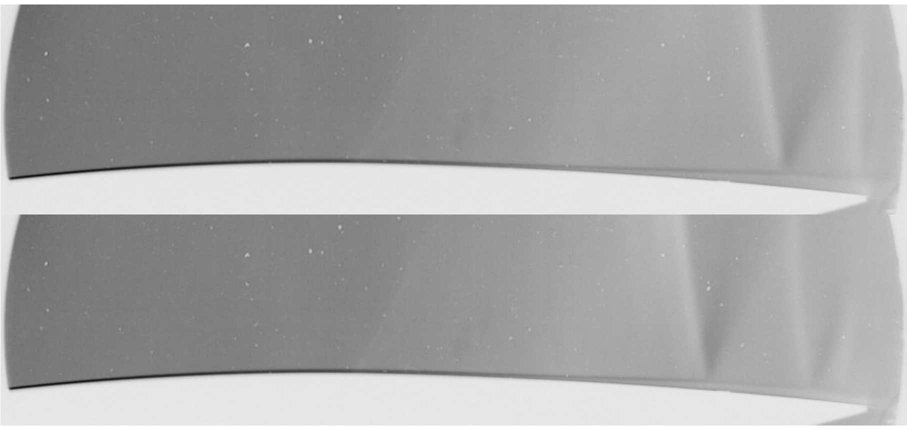

a) shaft position #1

b) shaft position #2

Figure 5 RMS of Schlieren intensity pulsations (P_0 = 0.3 bar)

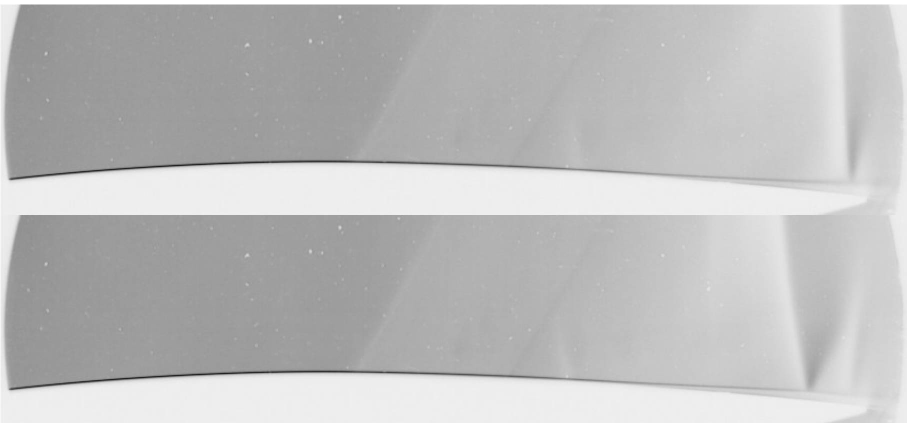

a) shaft position #1

b) shaft position #2

Figure 6 RMS of Schlieren intensity pulsations (P_0 = 0.7 bar)

Analysis of unsteady pressure data revealed only slight change of the pulsation spectra vs. spanwise coordinate. This means that spanwise distributions of unsteady parameters of the interaction are more or less uniform and the interaction can be considered quasi two-dimensional at least for scale $\lambda_z = 30$ mm, corresponding to parameter $\lambda_z/L = 4\div1$, (where L – length of the separation) depending on the shock intensity. Figure 7 presents the power spectra of pressure pulsations obtained in the symmetry plane at x =162 mm. The peak in the spectra was obtained for the shaft positions #1 and #2 and is associated with harmonic buffet oscillations. The presence of transonic buffet is confirmed by Schlieren visualization. Self-oscillations of the separation zone arose when the point of attachment reached the trailing edge. When the total pressure was changed from P_0 = 0.3 bar to P_0 = 0.5 bar the peak shifted to higher frequencies (from 0.8–0.9 kHz to 1.4–1.8 kHz). This effect is most likely linked to a decrease of the length of the separation zone. In addition increase of the total pressure is accompanied by the substantial growth of pressure pulsations in the entire frequency range, which indicates appearance of turbulence in the boundary layer at the point of measurement (x = 162 mm).

Figure 8 shows dependence of the cross-correlation between the sensor located in the symmetry plane (z = 0 mm) and the sensor placed at z = 18 mm. In the cases of extended separation (position #1 and #2) there is some periodicity in the plot that indicates the presence of two-dimensional harmonic oscillations of the shock wave and the flow separation point (buffet oscillation). However, there is a high level of coherence in range ±0.1 ms almost for all of the Mach numbers where the flow separation exists. This can be interpreted as two-dimensional shock wave oscillations with a spanwise extent at least about 30 mm.

Let's compare the auto-correlation of the central sensor with cross-correlations calculated for the same sensors (Figure 9). There is good agreement of the curves for buffet regime (shaft position #2) and non-harmonic oscillations (shaft position #3). This means that even for non-harmonic oscillations there is a high correlation of oscillations over a wide frequency range indicating existence of a quasi-2D pulsations. Perhaps powerful acoustic waves propagating upstream from the trailing edge (well visible on Schlieren imaging) are responsible for the existence of high level of pulsations correlation at different points on the model. When the separation reaches the trailing edge, the feedback appears leading to harmonic buffet oscillations.

DOI: 10.13009/EUCASS2017-350

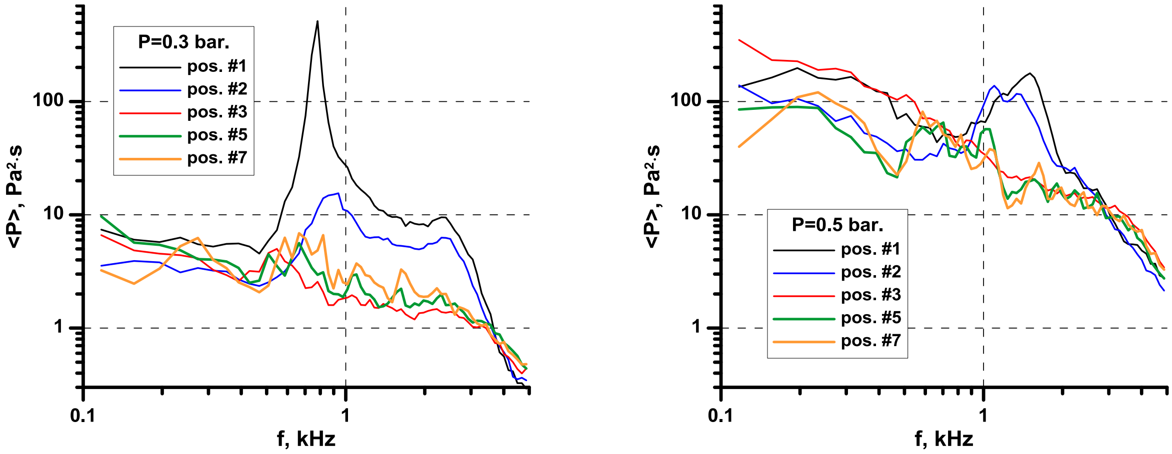

a) $P_0 = 0.3$ bar b) $P_0 = 0.5$ bar

Figure 7 Power spectra of pressure pulsations in the plane of symmetry

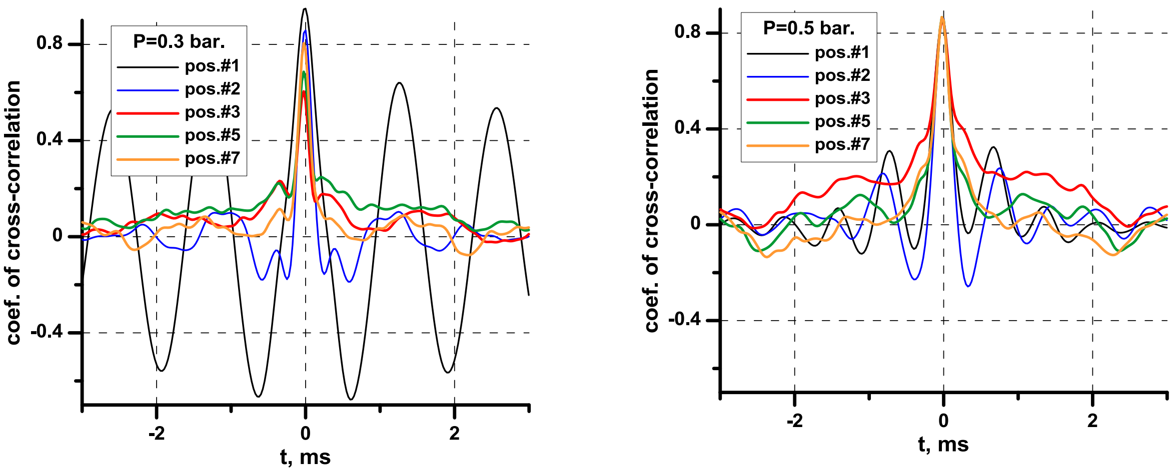

a) $P_0 = 0.3$ bar b) $P_0 = 0.5$ bar

Figure 8 Cross correlation for the pressure sensors at $z = 0$ and $z = 18$ мм

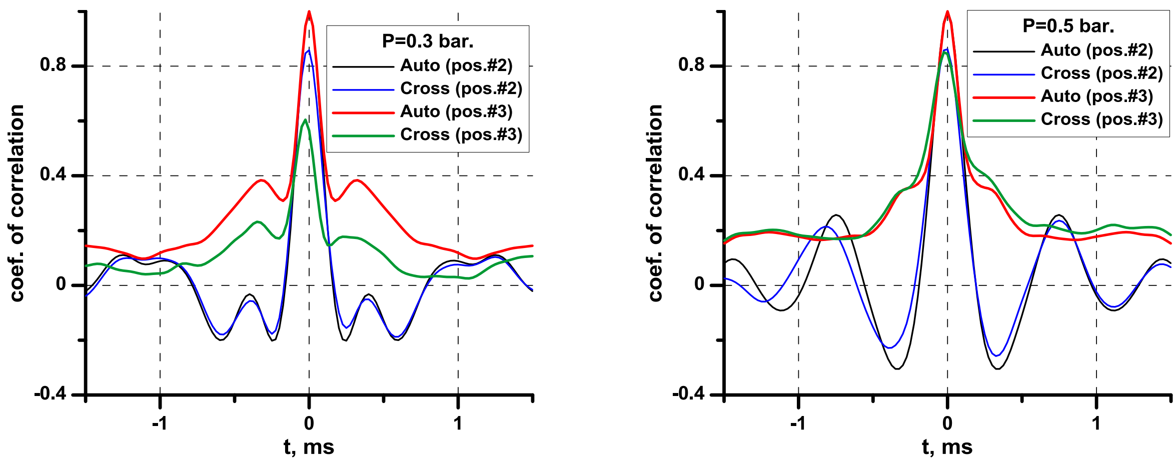

a) $P_0 = 0.3$ bar b) $P_0 = 0.5$ bar

Figure 9 Comparison of autocorrelation and cross-correlations

An example of the visualization demonstrating the plasma discharge effect on the flow is presented in Figure 10 and Figure 11. Activation of CDBD leads to substantial reduction of the separation zone. Analysis of the Schlieren series and the corresponding distributions of Schlieren intensity pulsations did not reveal the formation of turbulent spots

DOI: 10.13009/EUCASS2017-350

by the discharge. This means that CDBD actuator used in the experiment excites perturbations in the boundary layer, insufficient for sudden flow turbulization.

However, there is rapid growth of these disturbance in the zone of adverse pressure gradient and the shear layer, leading to earlier turbulization of the boundary layer, and consequently to reduction of the separation zone. It is necessary to note that no thermal spots were found in the Schlieren visualization. It means that the negative impact of such direct heat deposition in the flow is minimal. A significant reduction in the separation zone by activation of CDBD was allowed to suppress the laminar transonic buffet.

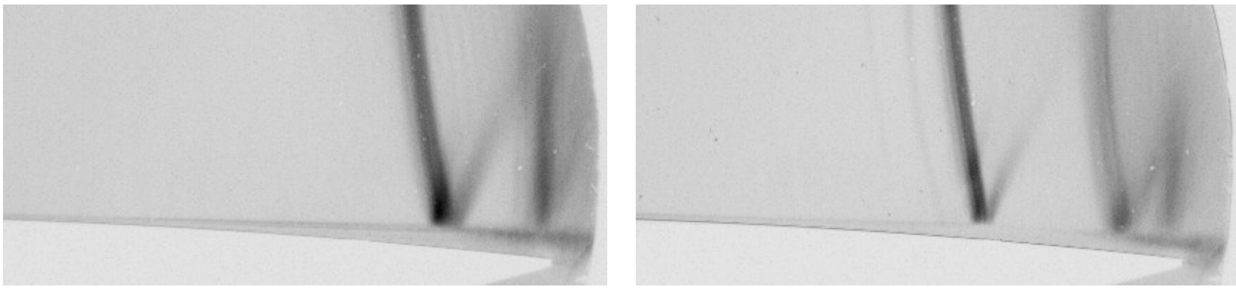

Referense case (plasma off)

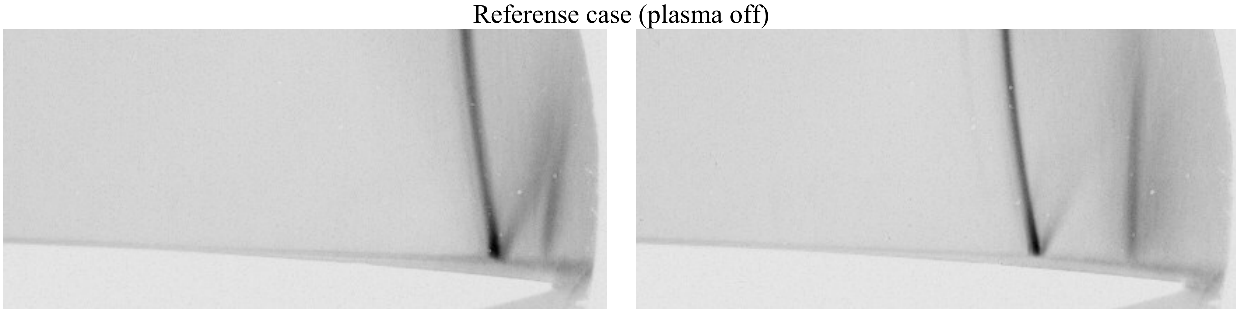

CDBD (plasma on)

a) shaft position #1 b) shaft position #2

Figure 10 RMS of the Schlieren image intensity pulsations (P_0 = 0.3 bar)

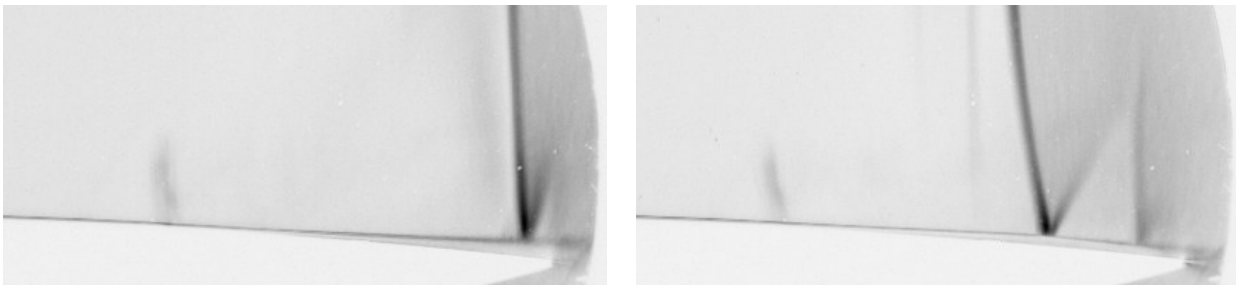

Referense case (plasma off)

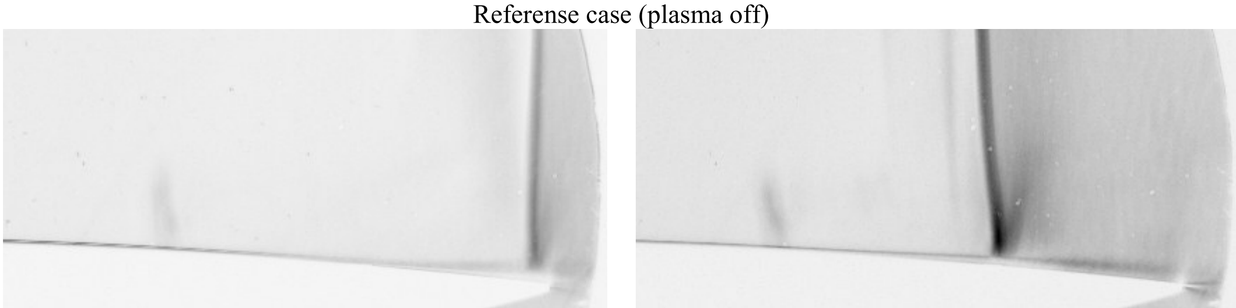

CDBD (plasma on)

a) shaft position #1 b) shaft position #2

Figure 11 RMS of the Schlieren image intensity pulsations (P_0 = 0.7 bar)

Effect of CDBD on the separated flow for different upstream Mach numbers is shown in Figure 12. The position of the shock wave and the point of the flow separation was found from the Schlieren visualization. Since for the laminar case the wave structure consists of several shock waves, only the position of the final shock wave was taken into account in the processing. Activation of CDBD leads to a weak shift of the final shock wave upstream. Experiments

DOI: 10.13009/EUCASS2017-350

with MSSD have been carried out in a wider range of pulse energy. The use of a powerful discharge allowed to rapidly turbulize the flow. As a result, the separated flow was completely suppressed, but the final shock wave shifted significantly upstream. This means that low-power CDBD should lead to more favorable distribution of pressure on the wing surface. Increasing the pressure from $P_0 = 0.3$ bar to 0.7 bar leads to substantial decrease of the separation zone with significant corresponding upstream shift of the final shock wave. This is a result of higher discharge power due to increased breakdown voltage with pressure rise (see Figure 12b) and correspondingly more powerful excited disturbances. Most likely, this leads to more rapid origination of turbulence in the zone of adverse pressure gradient. Significant reduction of separation leads to the disappearance of weak compression waves that might reduce the intensity of the final shock wave. Therefore, complete disappearance of the laminar flow separation is not optimal. Rather, there is an optimum of the discharge energy for each test case but the data do not allow to define it.

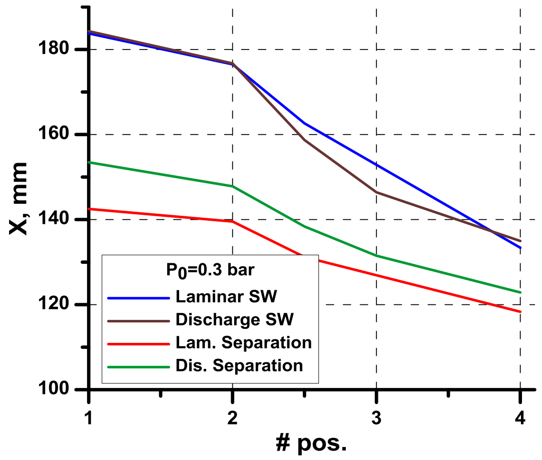

a) SW position ($P_0 = 0.3$ bar)

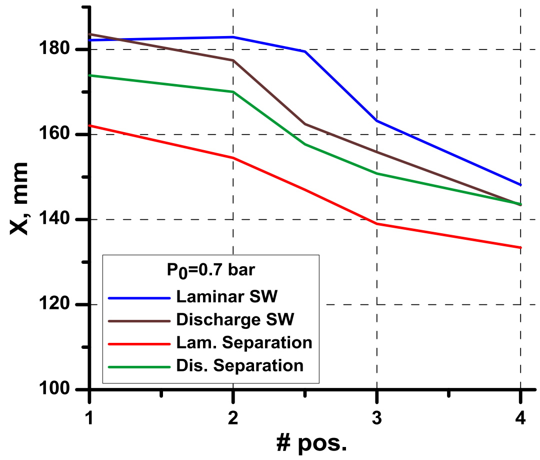

b) SW position ($P_0 = 0.7$ bar)

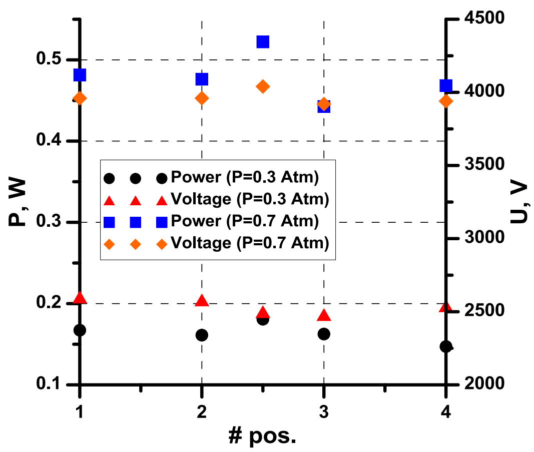

c) Discharge power

Figure 12 Effect of upstream Mach number on SW position (CDBD, $f = 13.4$ kHz)

Effect of the excitation frequency (in the range of characteristic interaction frequency) for two P_0 and two shaft positions is shown in Figure 13. An increase of the control efficiency with the frequency rise can be seen in the figure. Beyond the frequency $f_{mod} = 2$ kHz there is not any improvement the flow. Thus, it can be concluded that generation of the perturbations at a frequency of 3-4 times greater than the characteristic frequency of the interaction is sufficient for the control with minimum energy consumption. For example, for the test case of $P_0 = 0.3$ bar it is sufficient to use an average discharge power of 0.5 W/m.
The results presented in Figure 13c for low frequencies of 250 Hz and 500 Hz reveals the false trends, namely the constant power for continuously decreasing frequency, etc. The reason for this effect is bad statistics of the data acquisition.

DOI: 10.13009/EUCASS2017-350

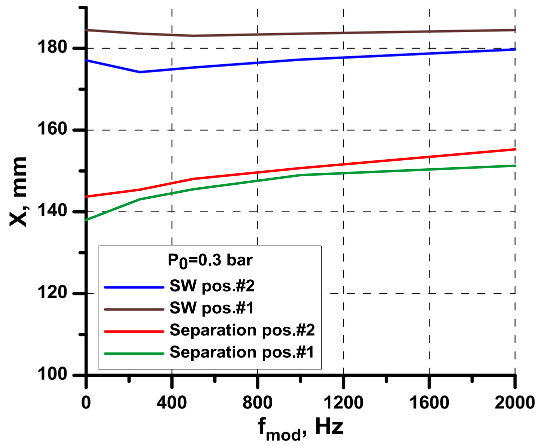

a) SW position, $P_0 = 0.3$ bar

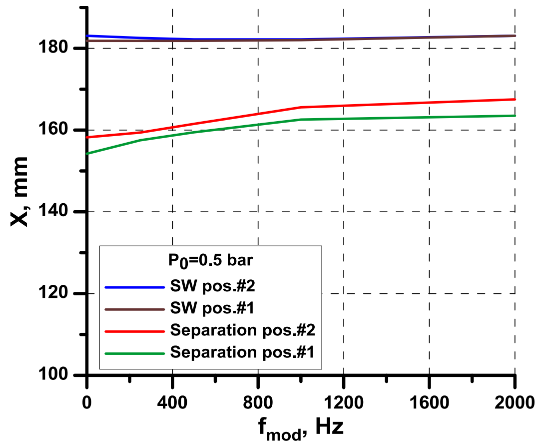

b) SW position, $P_0 = 0.5$ bar

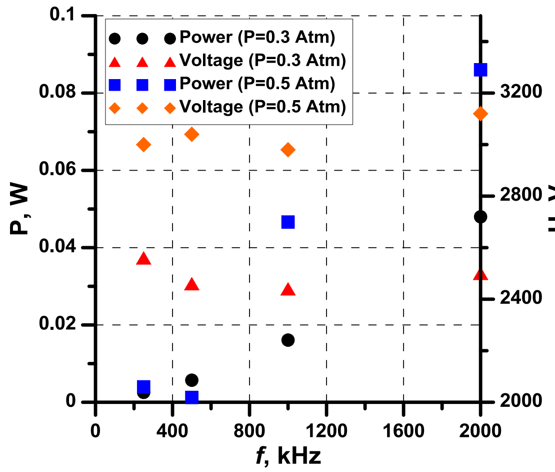

c) CDBD power

Figure 13 Effect of the CDBD excitation frequency on SW position

Figure 14 show the mean velocity distributions obtained for various frequencies (shaft position #2). Similar to the results of Schlieren visualization there were no difference observed between the cases of $f_{CDBD} =$ 13.4kHz and 5.2 kHz. Average power of CDBD during PIV measurements for the case of $P_0 = 0.3$ bar was 0.25W and 0.5W for the frequencies of 5.2 kHz and 13.4 kHz respectively.

It can be seen that activation of CDBD reduces the interaction zone, but maintains the flow structure the same. There is the flow acceleration beyond the first shock wave, followed by deceleration to subsonic speed at the final shock wave. These data give evidence that the total boundary layer turbulization does not occur until the end of the model. In the opposite case, the turbulization should significantly increase the boundary layer displacement thickness. This conclusion was confirmed by analysis of the boundary layer velocity profiles. The question about the mechanism of the interaction control by weak disturbances remains open.

DOI: 10.13009/EUCASS2017-350

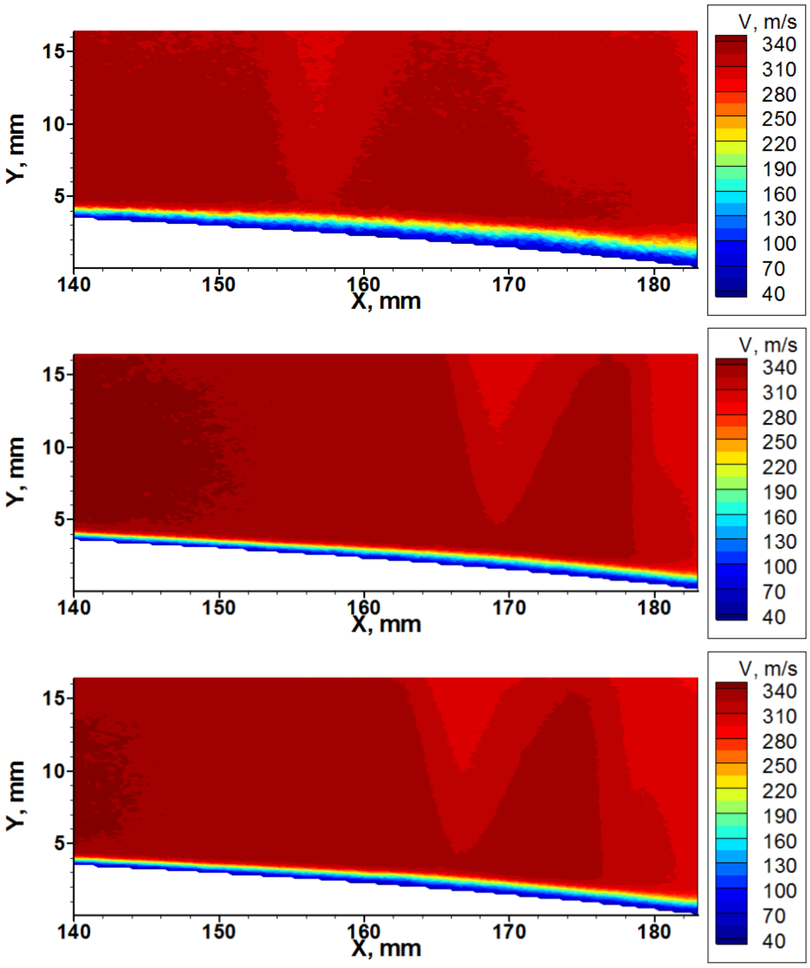

Laminar BL

CDBD f = 13.4 kHz

CDBD f = 5.2 kHz

Figure 14 Time averaged streamwise velocity distributions (shaft position #2, P_0=0.3 bar)

Estimation of the control efficiency in terms of the average flow parameters improvement was done as described below. An estimation of the energy losses in the interaction may be done basing on changes of the momentum thickness as $P_{los}=0.5\rho\cdot U^3(\theta_{lam}-\theta_{dis})$ (Figure 15). The curves corresponding to different frequencies of discharge completely coincide.

Figure 15 show that there is decrease of losses for the cases of plasma control in comparison to laminar reference case along the whole model. PIV data were obtained only for one Mach number (shaft position #2). Therefore, we cannot assert that the same effect would be obtained for lower Mach numbers where there is some degree of the flow turbulization due to movement of the shock wave upstream.

For the case studied, the maximum decrease of P_{los} was achieved near the trailing edge. For the total pressure P_0 = 0.3 bar this value is ≈550 W/m. Estimation of the control efficiency for the frequency 5.2 kHz gives a result $\eta_{dis}= P_{los}/P_{dis}$= 550[W/m]/(0.25[W]/0.1[m]) = **220** (or **22000%**). At the same time, we know from the Schlieren data that the flow pattern remains the same up to discharge frequency of 2 kHz. As a result for the lower frequency the efficiency is even higher $\eta_{dis}= P_{los}/P_{dis}$= 550[W/m]/(0.05[W]/0.1[m]) = **1100** (or **110000 %**). Taking into account the output-input ratio of the high voltage generator (about 35%) these values are **77** and **385 (7700%** and **38500%)** for the frequencies 5.2 and 2 kHz correspondingly.

In fact, for so low energy of the discharge its power consumption is negligible. Therefore the main disadvantage of plasma turbulators in front of the classical passive turbulators (such as roughness, vanes and so on) is diminished. Advantages of the turbulence control by plasma turbulators are connected with on-demand using and flexible control of the flow by variation of the discharge parameters.

DOI: 10.13009/EUCASS2017-350

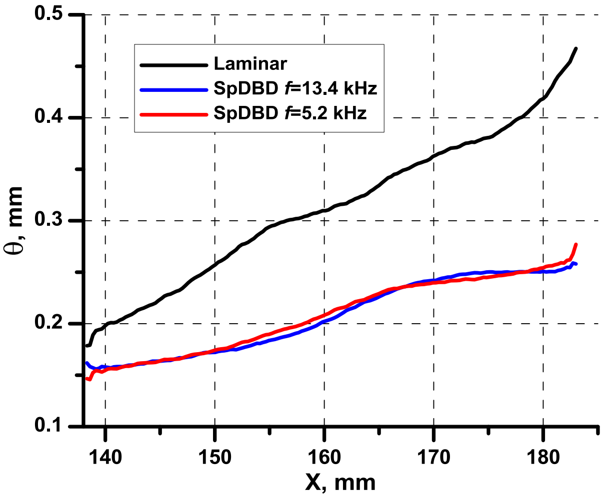

a) momentum thickness

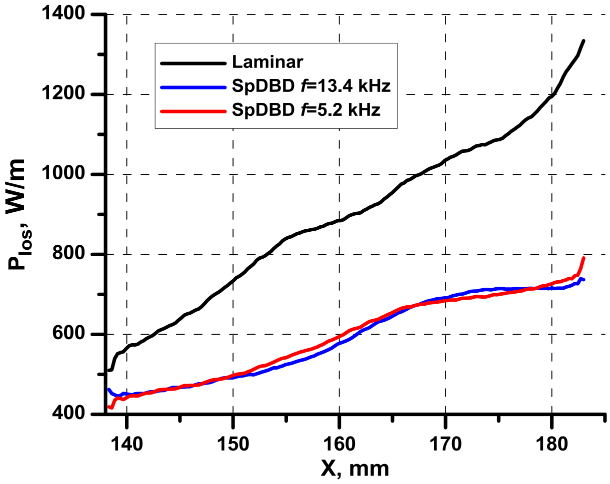

b) energy losses

Figure 15 Streamwise distribution of BL parameters and energy losses (shaft position #2, P_0=0.3 bar)

Conclusions

Two kinds of plasma actuators were developed and tested for the flow control by exciting the disturbances of low intensity in the flow, particularly Multi Sliding Spark Discharge and Contracted Dielectric Barrier Discharge. The experimental study of the effect of plasma actuators on the SWBLI on a laminar transonic aerofoil was carried out. Possibility of the separation flow control by these actuators has been demonstrated. The separation diminishing and complete elimination was achieved depending on the discharge power. Due to the disturbances generated by the discharge it is possible to achieve suppression of the buffet and to decrease the viscous losses in the zone of SWBLI. High efficiency of the separation control by plasma actuators was achieved in the experiments. The reasons of this are:

1) Low frequency and low duty cycle of the discharge (short pulse). This is a result the relatively long recovery time of the separation zone.
2) The energy in the pulse was close to the optimum, which is sufficient to generate perturbations at laminar boundary layer without creating a powerful thermal spot.
3) The plasma actuator was operated in single streamer discharge mode. This allows to localize the thermal energy in a small volume and intensify the generation of disturbances [11].

The electric discharge in contrast to the other types of turbulators (such as roughness) can make conditions similar to the beginning of a laminar-turbulent transition (low level of intermittence) along most of the wing surface. This makes it possible to form more favorable conditions for reducing the drag [5] in comparison with the classical turbulator.

The work was supported by Airbus under Research and Technology Contract and grant of Russian Foundation for Basic Research 16-08-01134A

References

[1] V. Brion, J. Dandois, S. Deck, L. Jacquin, P. Molton, Fulvio Sartor and D. Sipp. Transonic airfoil buffet: a decade of research at ONERA. XXIV ICTAM, 21-26 August 2016, Montreal, Canada.
[2] L. Jacquin, V. Brion, P. Molton, D. Sipp, J. Dandois, S. Deck, F. Sartor, E. Coustols, D. Caruana. Testing in Aerodynamics Research at ONERA: the example of the Transonic Buffet. 2016. Journal AerospaceLab. No.12.
[3] M. Diop, S. Piponniau and P. Dupont. On the length and time scales of a laminar Shock Wave Boundary Layer Interaction. 2016. AIAA Paper 2016-0073.
[4] R. H. M. Giepman, F. F. J. Schrijer, B. W. van Oudheusden. High-resolution PIV measurements of a transitional shock wave–boundary layer interaction. 2015. Exp Fluids 56:113. P. 20.
[5] P.A. Polivanov, A.A. Sidorenko, A.A. Maslov. Transition Effect on Shock Wave / Boundary Layer Interaction at M=1.47. AIAA Paper 2015-1974.

DOI: 10.13009/EUCASS2017-350

[6] J.-Ph. Boin, J.-Ch. Robinet. Three-dimensional unsteady laminar shock-wave / boundary layer interaction. 2004. NATO RTO-MP-AVT-111.

[7] G. Fournier, A. Chpoun and C. Tenaud. Shedding Intermittency in a Shockwave-Laminar Boundary Layer Interaction. XXIV ICTAM, 21-26 August 2016, Montreal, Canada.

[8] A. Lepage, J. Dandois, A. Geeraert, P. Molton, F. Ternoy, J.-B. Dor and E. Coustols. Transonic buffet alleviation on 3D wings: wind tunnel tests and closed-loop control investigations. 2017. Advances in Aircraft and Spacecraft Science. Vol. 4. No. 2. P. 145-167.

[9] W. Stalewski, J. Sznajder. Load control of natural-laminar-flow wing via boundary layer control. 2016. VII European Congress on Computational Methods in Applied Sciences and Engineering M. Papadrakakis, V. Papadopoulos, G. Stefanou, V. Plevris (eds.), ECCOMAS Congress 2016.

[10] Natural Laminar flow airfoil analysis and trade studies. Report NASA-CR-159029. 1979.

[11] P.A. Polivanov, A.A. Sidorenko, A.A. Maslov. Artificial turbulization of the supersonic boundary layer by dielectric barrier discharge. 2014. 29th Congress of the International Council of the Aeronautical Sciences.